# Post-synthetic Amide Insertion into Polyethylenes Augments Diverse Physical Properties and Enables Branching-dependent Recyclability


## Authors

Albert Ong[1] ‡, Jaime J. M. Pang[1] ‡, Loh Wei Wei[1], Jerald Y. Q. Teo[1], Li Ke[1], Xue Qi Koh[1], Tristan T. Y. Tan[1], Lewis Queh,[3] Zibiao Li[1,2,3]* and Jason Y. C. Lim[1,2]*

## Affiliations

[1] Institute of Materials Research and Engineering (IMRE), Agency for Science, Technology and Research (A*STAR), 2 Fusionopolis Way, Innovis #08-03, Singapore 138634, Republic of Singapore. E-mail: jason_lim@imre.a-star.edu.sg

[2] Department of Materials Science and Engineering, National University of Singapore (NUS), 9 Engineering Drive 1, Singapore 117576, Republic of Singapore

[3] Institute of Sustainability for Chemicals, Energy and Environment (ISCE[2]), Agency for Science, Technology and Research (A*STAR), 1 Pesek Road, Jurong Island, Singapore 627833, Republic of Singapore. E-mail: lizb@isce2.a-star.edu.sg

‡ These authors contributed equally to the manuscript.

## Abstract

Polyethylenes (PEs) possess unreactive saturated hydrocarbon backbones which make chemical recycling highly challenging, even at high temperatures. The insertion of strongly-hydrogen bonding amide linkages *into* the PE backbone can potentially confer recyclability via amide cleavage and reformation, whilst simultaneously bringing about new materials properties for functional upcycling. Herein, we demonstrate that in-chain amide insertion can be performed under a variety of reaction conditions, including the usage of *p*-cymene as a bioderived green solvent, with common and low-cost reagents, on both high-density (HDPE) and low-density PEs (LDPE). ~1 amide bond/ 100 ethylene repeating units can enhance not only the polymers' tensile properties, but also elicit unexpected increase in surface hydrophobicity and solid-state clusteroluminescence that was absent in the parent PEs. Additionally, we uncover the hitherto-overlooked importance of PE structure on their chemical recyclability. While low-branching amide-containing HDPE could be hydrolysed and reformed for three cycles at ≤150 °C without compromising their tensile properties, attempted chemical recycling of highly-branched LDPE formed a thermoset-like crosslinked polymer with greatly enhanced ductility. Our findings showcase amide-insertion as a versatile means to access new functional applications that are originally inaccessible to PEs without requiring additives, with branching-dependent influences on chemical recyclability for circular polymeric materials design.

## Introduction

Polyethylenes are extremely versatile and low-cost plastics, whose annual production exceeds 100 million tonnes. Their utility and popularity across diverse applications stems from their wide range of material properties accessible, such as density, ductility, tensile strength, melt point, and resistances toward chemicals and solvents,[1, 2] governed by differences in polymer branching and molecular weight. Despite their ubiquity, the vast majority are disposed by incineration and landfilling at their end-of-life, with only a small percentage subjected to mechanical recycling. Unlike closed-loop chemical recycling which allows regeneration of virgin polymers, mechanical recycling causes inevitable material degradation after repeated iterations due to unavoidable oxidation and chain cleavage.[3] However, in contrast to cleavable bond-containing polymers such as polyesters, chemical recycling of PE remains highly challenging and largely impractical due to their unreactive saturated hydrocarbon backbones. Thus, high temperatures exceeding 700 °C are often required, affording low ethylene monomer recovery (<30%) with extensive formation of complex mixtures of oligomeric hydrocarbon by-products.[4] Enabling chemical recycling under milder conditions allows better control of depolymerisation pathways, reduced likelihood of thermal decomposition and improved monomer recovery yields for subsequent repolymerisation.

In light of that, chemically-recyclable PE-like polymers can be engineered by incorporating cleavable ester linkages at point-of-synthesis, either through radical ring-opening polymerisation of cyclic ketene acetals[5] or via polycondensation of plant oil-based monomers[6]. Additionally, polyethyleneketones synthesised by ethylene-CO copolymerisation offer opportunities for post-synthetic modification, where the incorporated carbonyl groups are reactive sites for conversion to esters and amides[7, 8]. While promising, these methods require the synthesis of specialised monomers, sourcing of alternative feedstock of higher cost, as well as significant remodelling of industrial synthesis procedures that can invoke higher capital and operational expenditures. Recently, post-synthetic insertion[9] of cleavable esters and amides [10-12] into the polymer backbone of PEs offered new opportunities to transmutate them into closed-loop recyclable polymers. Compared to the aforementioned alternatives, post-synthetic skeletal editing offers several advantages: First, it can be performed on PEs at any stage of their life cycle – being equally feasible on virgin or end-of-life PEs; Next, this minimises disruptions to existing industrial-scale PE production, as skeletal editing can occur post-synthesis; Finally, the same skeletal editing procedure can be performed on the vast variety of PEs already available (e.g. LDPE, HDPE). This allows convenient access to a range of polymers without

the need for new polymerisation procedures and feedstock to achieve the material diversity that gives PEs their versatility.

The grafting of different polar functional groups (e.g. hydroxyl, carbonyl, amides) onto the barren saturated hydrocarbon PE backbones can confer new properties such as enhanced adhesiveness and water miscibility[13-15], significantly expanding the range of applications that were previously inaccessible to PE. However, the saturated PE backbone remains fundamentally unchanged in these cases, preventing chemical recyclability and potentially complicating the fate of these upcycled polymers at their respective end-of-lives. This inspired us to explore the possibility of modifying PEs with hydrolysable amide linkages, to simultaneously enable both improved physical properties,[8] as well as chemical recycling, to close the material loop. Amides are capable of strong hydrogen bonding, which exerts dominant structure-directing influences on nylons[16, 17] and confers unique properties in polyacrylamides.[18] Furthermore, polyamides are susceptible to hydrolytic depolymerisation at temperatures much lower than that required for PE pyrolysis (≤200 °C).[19, 20] Thus herein, we demonstrate the unique and unexpected effects of inserting amide linkages post-synthetically *into* the backbone of both high density (HDPE) and low density polyethylenes (LDPE), via scalable Beckmann rearrangement reactions, on the polymers' physical properties and chemical recyclability (**Figure 1**). With even a small amount of amide linkages (~1 amide for every 100 ethylene repeating units) present, up to ~3-fold increase in maximum elongation at break was observed. Unexpectedly, insertion of these polar bonds could *increase* the surface *hydrophobicity* of the resulting polymer films compared to their parent PEs, and bring about polymer luminescence that was originally absent. Indeed, the ability of this simple chemical transformation to confer new properties to PEs is advantageous to the conventional usage of additives, which can complicate waste streams and post-use plastic treatment[21, 22], and can pose hazards to the environment and human health.[23, 24] Other than these physical properties, we highlight the unexpected, yet completely different chemical recycling outcomes associated with the PE polymer structures: While amide-inserted HDPE (HDPEAm) could be hydrolysed and repolymerised repeatedly for at least three times, the corresponding modified LDPE polymer (LDPEAm) formed a thermoset-like crosslinked polymer upon repolymerisation.

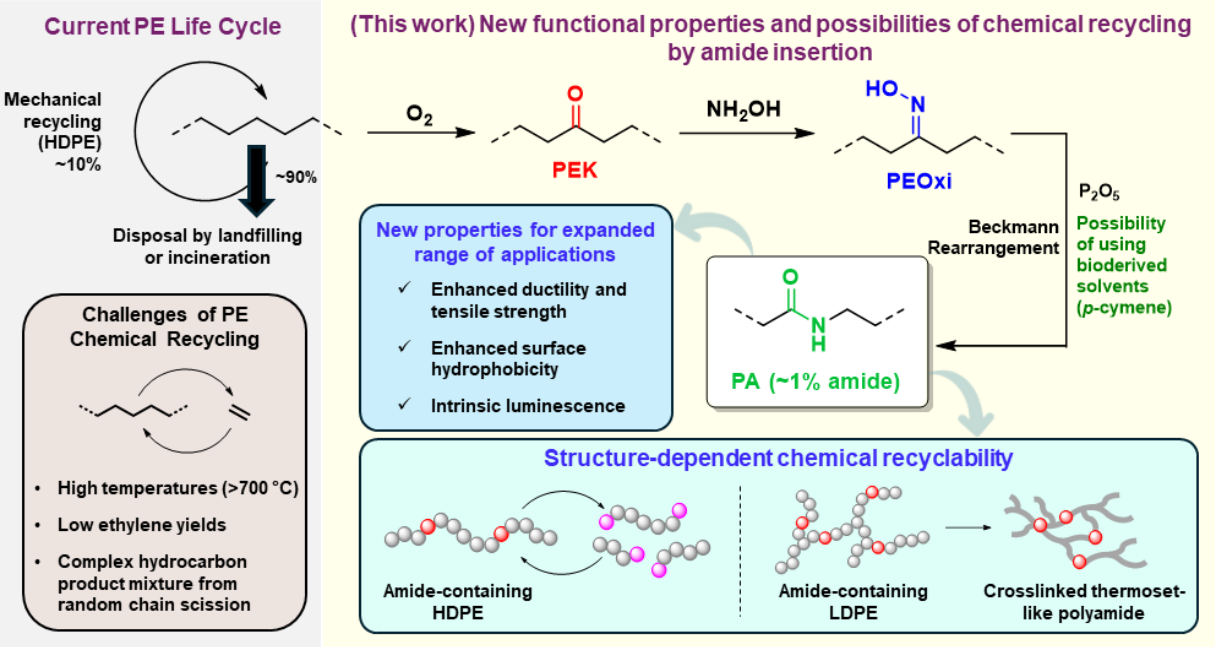


**Figure 1.** Schematic illustration showing that post-synthetic amide insertion into the backbone of PEs confers new functional properties, whilst resulting in structure (branching)-dependent chemical recyclability.

## Results and Discussion

### Enhancement of Diverse Physical Properties after Amide Insertion into PEs

To insert amides *into* the PE backbone, the polymer was first oxidised to append carbonyl groups onto the hydrocarbon chain, followed by Beckmann rearrangement using low-cost, industrially-relevant reagents (**Figure 1**). LDPE and HDPE were both subjected to post-synthetic amide insertion to demonstrate the feasibility of these modifications on structurally-distinct PEs, and to elucidate the impact of their structure on subsequent chemical recyclability (*vide infra*). LDPE oxidation was achieved by benzaldehyde-mediated aerobic oxidation to form the polyethyleneketone (LDPE-K),[25] installing carbonyl groups exclusively (~1% functionalisation), evident from the dominant triplet signal at 2.39 ppm in the $^{1}$H NMR spectra (**Figure 2a**, see **Figure S6** for full spectrum). Their presence was further corroborated by characteristic $^{13}$C NMR signals (211.2 ppm) (**Figure S7**) and FTIR C=O stretching frequency (1720 cm$^{-1}$) (**Figure 2b**). Notably, benzaldehyde-mediated LDPE oxidation did not introduce hydroxyl groups on the methylene protons of the polymer backbone, evident from the absence of $^{1}$H NMR signals around 3.6 ppm.[26] Similarly, formation of tertiary hydroxyl groups on the LDPE branch points (not detectable via $^{1}$H NMR spectroscopy) were also not observed, from

the absence of detectable α-hydroxyl $^{13}$C NMR signals between 45-75 ppm in both TCE-$d_2$ or toluene-$d_8$ (**Figures S7 – S8**). For HDPE, as benzaldehyde-mediated oxidation resulted in low carbonyl functionalisation, we employed an alternative organocatalytic C-H aerobic oxidation method catalysed by commercially-available tetrachloro-*N*-hydroxyphthalimide ($Cl_4$-NHPI), which afforded ~2% carbonyl functionalisation on the resulting HDPE-K.[27, 28] Like LDPE oxidation, carbonyl insertion was dominant, though small quantities of hydroxyl and chloro functionalisation (<0.1%) were also observed (**Figure S17, S18**). For both LDPE-K and HDPE-K, the absence of $^1$H NMR signals at ~2.7 ppm that corresponded to closely-spaced carbonyl groups[29], indicated that the inserted C=O bonds are not located close to each other, but are likely randomly positioned along the polymer chain separated by significant lengths of methylene segments.

Thereafter, the polyethyleneketones were condensed with hydroxylamine hydrochloride to form oxime intermediates, which are then subjected to Beckmann rearrangement using $P_2O_5$ that functioned both as an acid and a dehydrating agent. Due to the excellent solvent tolerance of the polyethyleneketones, these transformations were initially performed in 1,2,6-trichlorobenzene (1,2,4-TCB). Both LDPEK and HDPEK were converted to their respective oximes with 93% and 75% conversions respectively. Unlike carbonyls, the α-protons of oximes are chemically distinct, and are observed at 2.19 and 2.36 ppm (TCE-$d_2$) (**Figures 2a, S9 and S20**). Likewise, the appearance of the oximes' characteristic $^{13}$C NMR signal (*C*=N-OH) at 162.9 ppm[30] (**Figures S10 and S21**) is indicative of its formation. Subsequently, Beckmann rearrangement was successfully performed on the PE-oximes, converting them to LDPEAm and HDPEAm, containing 0.84% and 0.96% amide functionalisation respectively (**Figures S11 and S22**). Their presence was indicated by the replacement of the oxime $^1$H NMR signals with new signals corresponding to the amide α-protons: a quartet at 3.25 ppm (C*H*$_2$-NHCO-) and a triplet at 2.15 (NHCO-C*H*$_2$-) (**Figure 2a**); as well as the diagnostic $^{13}$C NMR amide carbonyl signal at 172.9 ppm (**Figures S12 and S24**). Better carbonyl-to-amide conversions were obtained for LDPE compared to HDPE, largely due to the superior solubility of the LDPE derivatives, allowing the sequential transformation reactions to be performed at lower temperatures that reduced the likelihood of side reactions occurring, particularly in the presence of highly reactive $P_2O_5$. Indeed, under the conditions for Beckmann rearrangement of HDPEOxi at 120 °C, several additional signals corresponding to unidentified functional groups were observed (**Figures S22 – S23**), which were not seen for the corresponding reaction for LDPEOxi at 65 °C (**Figure S11**). Regardless of this, the multi-

stepped amide insertion process yielded mainly amide linkages in the final polymers for both HDPE and LDPE, which is notable considering that errors in skeletal editing are often structurally encoded permanently into the polymer product. Comparing the resulting polymers' $^{1}$H NMR amide α-proton signals with that of an aliphatic model amide (**Figures 2a and S1**) indicates that the amide linkages inserted into PE are well-separated from each other on the hydrocarbon chain, as expected from the grafting of spatially-separated carbonyl groups aforementioned. Additionally, the amide-carbonyl FTIR stretches at 1647 and 1649 $cm^{-1}$ for LDPEAm and HDPEAm (**Figures 1c and S36**) respectively are indicative of disordered hydrogen bonded carbonyl groups,[31] further supporting the random amide positioning which can disrupt chain packing regularity,[32] with implications on material properties (*vide infra*).

Performing the post-synthetic amide insertion in a homogeneous phase enables dispersal of the polymer in the solvent, facilitating access of reagents to reactive sites for chemical transformations to occur. However, the known solvent resistance of PEs restricts the range of usable solvents to either health- and environmentally-hazardous aromatic or chlorinated solvents.[7, 26, 33, 34] To improve the sustainability of amide insertion reactions, we thus explored replacing 1,2,4-TCB with *p*-cymene, a biorenewable solvent obtained as a by-product of citrus fruit processing [35, 36] and has been used as a sustainable alternative to conventional aromatic solvents, even on industrial scales. [36-39] Both HDPEK and LDPEK were found to be miscible with *p*-cymene when heated, allowing high degrees of conversion (~80%) (**Figures S14 and S31**) to the oximes under identical conditions as 1,2,4-TCB. Similarly, higher degree of transformation to amides (93%) was achieved with LDPEOxi compared to HDPEOxi (66%), obtaining polymers containing 0.8% and 1.0% amide functionalisation respectively (**Figures S15 and S32**), owing to the latter's poorer solubility which required higher temperatures for miscibility. While the initial oxidation of HDPE to HDPEK could not be performed using *p*-cymene due to the possibility of solvent oxidation[40], this reaction can also be mediated by benzaldehyde, obtainable from biomass sources[41], albeit with lower degrees of carbonyl functionalisation (**Figure S16**). Together with our usage of readily-available, low-cost reagents, our findings suggest the possibility of performing such post-synthetic amide insertions under sustainable, potentially-scalable batch reaction conditions.

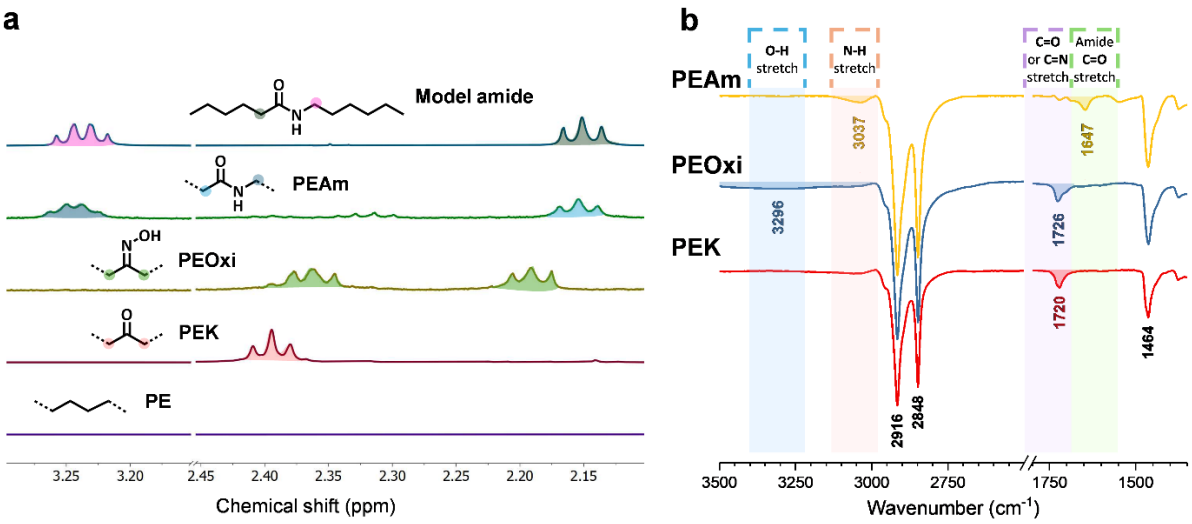


**Figure 2. a)** Stacked $^{1}$H NMR spectra (TCE-$d_2$) showing the diagnostic signals corresponding to intermediates during insertion of amides into LDPE. **b)** FTIR spectra of LDPE-derived ketone, oxime and amide.

Analyses of the PEs' molecular weight changes after insertion of amide linkages by high temperature GPC revealed reduction in their molecular weights, with a greater extent of chain cleavage observed for HDPE compared to LDPE (**Table 1, Figure S37**). This suggested the possibility of changes in the structure of the parent PEs during the amide insertion process. To ascertain that HDPEAm and LDPEAm retained their low and high extents of branching after amide insertion, we performed $^{13}$C NMR analyses to identify characteristic resonances arising from the various carbon environments around branch-points (**Figures S33 – S34**).[42] Aerobic oxidation of LDPE to LDPEK, oxime formation and Beckmann rearrangement to form LDPEAm retained all the characteristic signals from 1°, 2° and 3° carbon positions that were originally present in the parent LDPE (**Figure S33**). Similarly, the $^{13}$C spectra of HDPEAm and the intermediates did not show detectable evidence of new methine (-CH-) signals that would indicate additional branch formation (**Figure S34**)[43]. Thus, amide-insertion into the PE backbones can largely retain the branching intrinsic to the parent polymer, in spite of their observed molecular weight reduction.

The effects of amide insertion on PE properties on the tensile properties of the resulting polymers were first determined in comparison with their parent PEs. Even a small degree of amide insertion (~1 amide/100 repeating units) was sufficient to bring about significant increases in ultimate tensile strength, elongation and maximum stress at break (**Figure 3a,**

**Table 1**), with similar Young's modulus as the parent polymers. A greater extent of tensile property enhancement was observed for LDPEAm than HDPEAm compared to their parent PEs. For instance, amide insertion could increase LDPE's ultimate tensile strength and strain at break by ~1.5- and ~3-fold respectively. However, HDPEAm only showed a ~1.1-fold and ~1.3-fold enhancement in the same parameters respectively compared to HDPE. We observed that the polymer concentration during the $P_2O_5$-mediated Beckmann rearrangement could influence the mechanical properties of HDPEAm: a HDPEOxi concentration of 0.04 g/mL afforded HDPEAm with the aforementioned enhanced tensile properties, whilst higher concentration of 0.057 g/mL resulted in brittle polymers (**Figure S42**). It is noteworthy that unlike ester incorporation which can result in poorer tensile behaviour,[44] amide insertion resulted in the opposite effect. Even with a considerable reduction in molecular weight after amide insertion, enhancement of tensile properties for HDPEAm remain observable and significant.

**Table 1.** Changes in physical properties of polymers after amide insertion into HDPE and LDPE.

| **Property** | **HDPE** | **HDPEAm** | **LDPE** | **LDPEAm** |
|---|---|---|---|---|
| $M_n$/ kDa [a] | 8.4 | 4.0 | 6.2 | 5.4 |
| $M_w$/ kDa [a] | 125.1 | 41.1 | 70.1 | 52.5 |
| PDI [a] | 15 | 10 | 11 | 9.8 |
| $T_c$ /°C [b] | 113.5 | 85.4 | 78.5 | 70.4 |
| $T_m$ /°C [b] | 129.2 | 111.5 | 94.4 | 93.9 |
| $T_d$ /°C [c] | 461.8 | 434.4 | 438.5 | 453.9 |
| Ultimate tensile strength /MPa [d,e] | 14.34 ± 0.24 | 16.33 ± 0.57 | 5.98 ± 0.09 | 8.38 ± 0.81 |
| Elongation at break /% [d,e] | 87.2 ± 16.4 | 117.2 ± 17.8 | 30.4 ± 3.0 | 102.1 ± 5.5 |
| Max stress at break /MPa [d,e] | 11.98 ± 0.60 | 13.78 ± 0.88 | 5.94 ± 0.05 | 8.17 ± 0.81 |
| Young's Modulus /$10^8$ Pa [d,e] | 2.66 ± 0.31 | 2.72 ± 0.58 | 1.19 ± 0.42 | 0.92 ± 0.14 |
| Water contact angle/° [e] | 88.3 ± 0.4 | 103.7 ± 2.2 | 100.8 ± 2.0 | 106.5 ± 2.3 |

Determined via [a]high-temperature GPC analyses, with molecular weights determined against polystyrene standards, polydispersity index (PDI) = $M_w$/ $M_n$; Determined by [b]DSC and [c] from the extrapolated onset temperatures from the TGA curve; [d]Determined from tensile analyses;

[e]values are the averages of three repeats. See Supporting Information for details of the respective analyses.

To elucidate the influences of amide hydrogen bonding on the PEs' tensile properties, molecular dynamics (MD) and density functional theory (DFT) simulations were performed on a linear HDPE model containing 200 repeating methylene units[45]. DFT modelling indicates that with just 1% backbone amide incorporation, the binding strength between the oligomers increased significantly as a result of NH···O hydrogen bonding between interchain amide groups that was not possible in HDPE model (**Figure 3b, Section S14**). This contributed to a higher degree of cohesional entanglement from non-covalent interactions between neighbouring chain segments (**Figure S57e**).[46] Upon stimulated deformation of HDPEAm oligomers, the average number of hydrogen bonds decreased from 1.6 to 1.4 per chain (**Figure S57f**), resulting in energy dissipation that accounts for the higher toughness and ultimate tensile strength observed in HDPEAm. At the same time, computational analyses indicated that 1% amide incorporation results in a decrease in polymer crystallinity (**Figure S57a, Supporting Information**), which was corroborated by XRD analyses showing a reduced ratio of integrated intensities between the crystalline and amorphous domains (**Figure 2c and S45 – S48, Supporting Information**). This indicated that the inserted amides disrupted the PEs' orthorhombic crystal structure[47], likely due to a combination of 'kink' formation that disrupted chain packing regularity and additional hydrogen bonding, further corroborating the aforementioned amide-carbonyl FTIR stretches indicative of disordered hydrogen bonded carbonyl groups (**Figures 2b, S36**). From the surface topology of the annealed HDPEAm dog-bone specimens via AFM (**Figure 4a or S51)**, both amorphous and lamellar structures were present, which contrasts with the regularly-distributed lamellae (~30 nm) seen for HDPE with its higher degree of crystallinity (**Figure S49**). The resulting two-phase morphology with semi-crystalline domains dispersed in an amorphous matrix which contributes to the excellent mechanical properties of HDPEAm, which has also been observed for different polyamide systems.[32, 48, 49] Compared to HDPEAm, the observed greater enhancement in tensile properties of LDPEAm compared to the parent polymer may be attributed to contributions from both higher polymer molecular weight, as well as the influences of branching on cohesional entanglement brought about by NH···O hydrogen bonding, and topological entanglement between polymer chains.[46, 50]

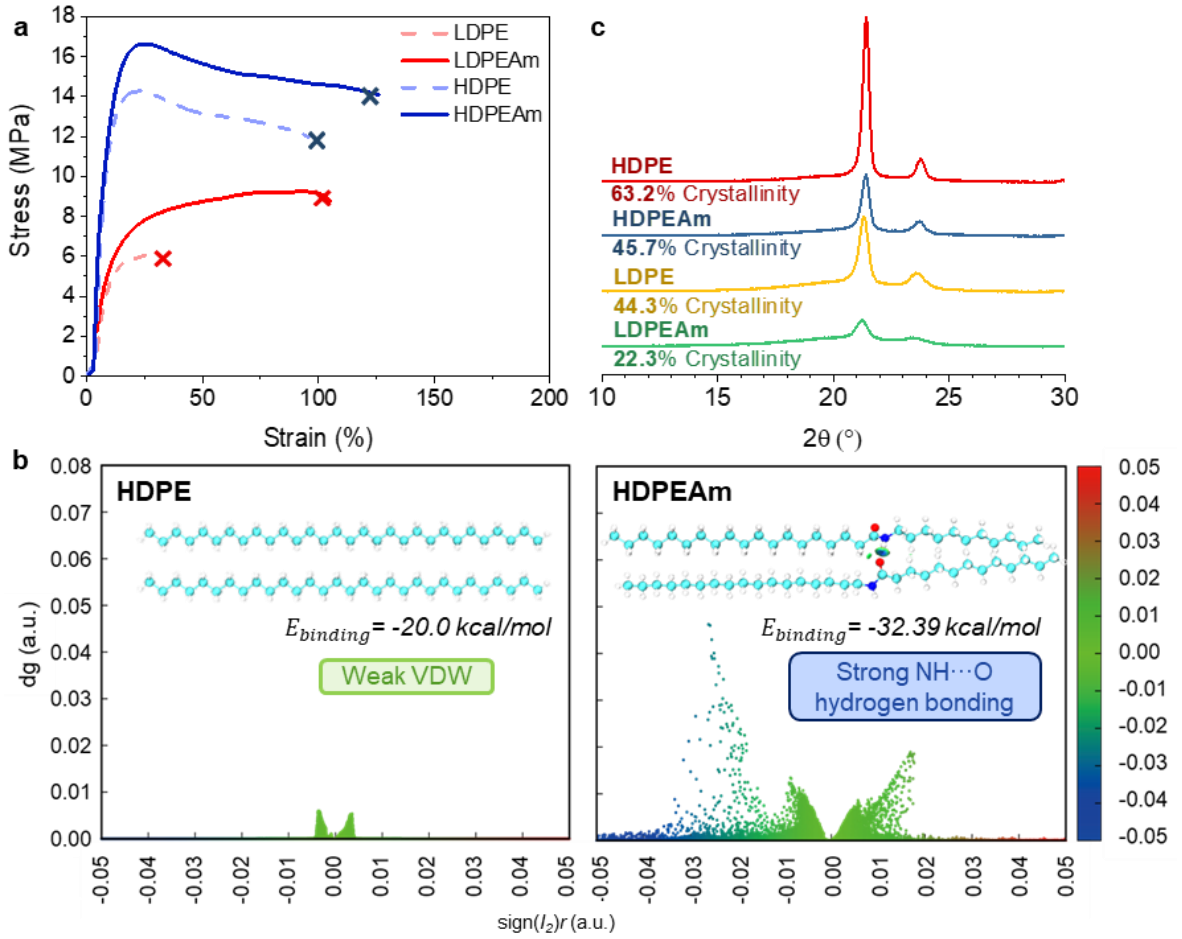


**Figure 3**. **Material characterisation of HDPEAm and LDPEAm specimens. a)** Stress-strain curve of the PE-derived polyamides (solid lines) compared to the original PE polymers (dashed lines). **b)** Scatter maps of $\delta g^{inter}$ versus $sign(\lambda_2)\rho$ of interacting HDPE (left) and HDPEAm (right) oligomers, with their optimised structures and sign($\lambda_2$)ρ colored $\delta_g^{inter}$ isosurface maps (Independent gradient model based on Hirshfeld partition analyses via Multiwfn)[51-63]. **c)** Stacked powder XRD analyses showing changes in crystallinity of PEs upon in-chain amide insertion. All analysis samples were fabricated materials processed with the same method (refer to **Figure S45 – S48** for the processing method, Supporting Information).

Amide insertion into the PE backbone was found to bring about unexpected changes in the surface hydrophobicity of HDPEAm and LDPEAm compared to their PE precursors. Although the inclusion of polar amide linkages is expected to increase polymer hydrophilicity, water contact angle (WCA) measurements performed on annealed dog-bone specimens (**Figure 4b and S43**) showed an *increase* in surface hydrophobicity for both HDPEAm (ΔWCA = ~15°) and LDPEAm (ΔWCA = ~6°). Comparing the surface granularity of HDPE and

HDPEAm dog-bone specimens indicated a possible origin of this phenomenon (**Figure 4c**): HDPEAm possessed ~8.8 times more grains detected with a total detected granularity area ~3.7 times more than HDPE. More extensive granularity suggest that HDPEAm's enhanced microscale roughness could enhance surface hydrophobicity[64] via a 'pseudo-lotus effect', akin to the villi-structured papillae of lotus leaves eliciting superhydrophobicity.[65] This may be attributed to the random, sporadic locations of the amide linkages in the polymer chain, whose NH···O hydrogen bonding induces irregular chain folding by alignment of hydrophobic polymer segments to form surface protrusions upon annealing. The greater increase in hydrophobicity upon amide insertion to HDPE compared to LDPE may be a consequence of the former's originally more regular polymer packing, where AFM imaging showing that lamellar structures indicative of ordered alignment of polymers in crystalline domains were observed for HDPE but not LDPE (**Figure S49 – S50**), leading to a greater change in surface roughness upon polymer skeletal editing. Our observed enhancement of polymer surface hydrophobicity from low extents of in-chain amide linkage insertion contrasts with polyamides comprising of regularly-spaced amide linkages, which are more hydrophilic than PE.[66] Additionally, this also differs from the increase in hydrophilicity reported when amides are appended *onto* the PE backbone, even if these appended amides themselves contain hydrophobic aryl groups[67]. The measured WCA for our PE-AMs are similar to those of fluorinated polymers such as PTFE[68] or PVDF[69], suggesting that these modified PEs may be potential replacements (for water resistive applications) for these fluorinated polymers that can release PFAS when degraded.[70]

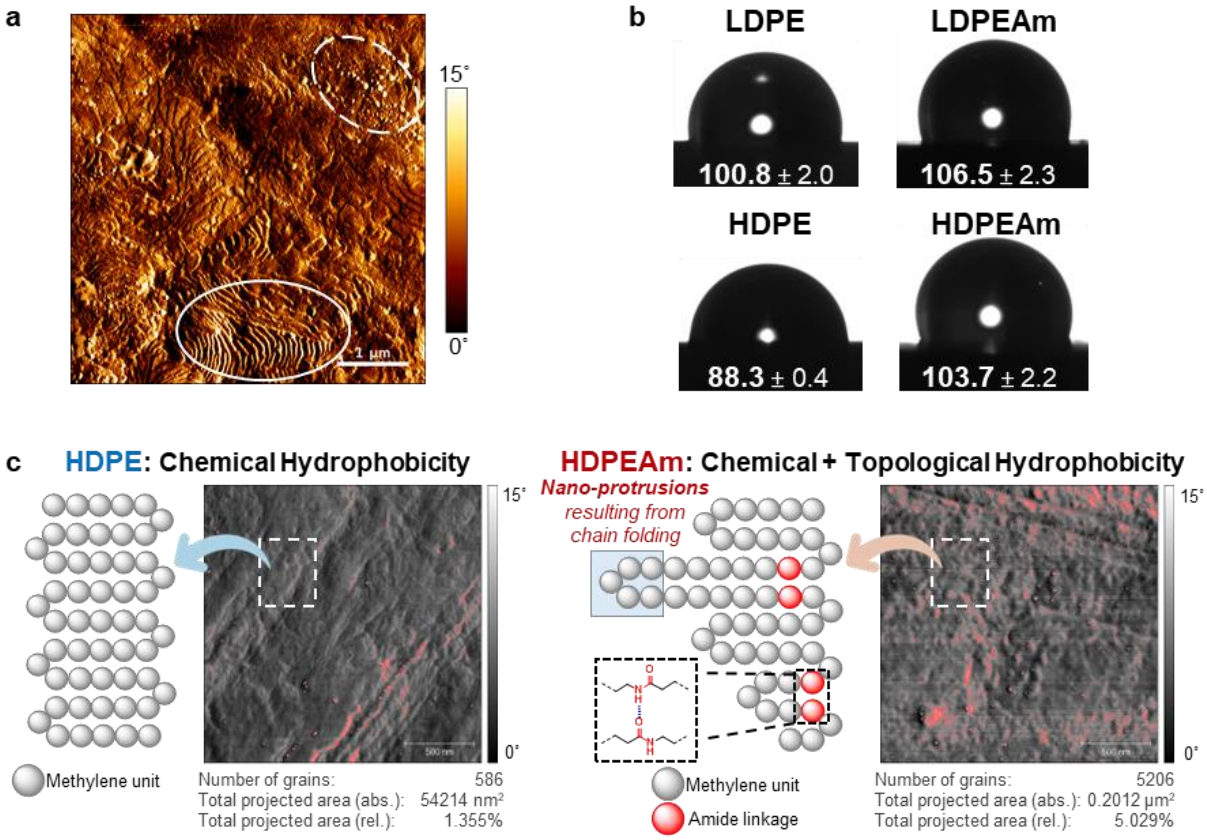


**Figure 4**. **Surface analyses of HDPEAm and LDPEAm specimens. a)** AFM phase image of HDPEAm (5 x 5 µm) depicting lamellar structures (solid circle) and micro-roughness resulting from irregular agglomeration of the polymer chains (dashed circle). **b)** Water-contact angles of LDPE, LDPEAm, HDPE and HDPEAm. **c)** Granularity of HDPE and HDPEAm surface quantified using particle analysis of the phase images of HDPEAm and HDPE surfaces by a threshold (45%) detection method. Red shaded area denotates detected grains. The formation of micro-protrusions on the HDPEAm surface due to hydrogen bonding of randomly spaced in-chain amides is depicted.

Having established the effects of in-chain amide insertion on the mechanical and surface hydrophobicity on PEs, we next investigated if their presence can alter the luminescent properties of the polymers. When excited at 390 nm, HDPEAm and LDPEAm containing ~1% in-chain amide linkages showed visible luminescence detectable by the naked eye (**Figure 5a**). The emission spectra of the PEAm polymers recorded in suspension in either toluene or TCB at 25 °C at 1 mg/mL ($\lambda_{ex}$ = 390 nm) showed emission peaks at 442 nm and 495 nm in toluene and TCB respectively (**Figure 5b**). Under identical conditions and concentrations, the parent PEs showed no detectable emission (**Figure S52**), clearly indicating that the observed

fluorescence did not originate from any trace additives that may be present in the PE precursors. Significant but less intense emission peaks were observed at lower and higher wavelengths (**Figure 5b**), suggesting the possible presence of different emissive species. When warmed to 50 °C, dissolution of the polymers in toluene at the same concentration resulted in complete loss of fluorescence (**Figure 5c**). The detectable fluorescence in the solid state, but not when dispersed in dilute solution, is consistent with fluorescence originating from the clusterisation triggered emission (CTE) mechanism[71]. Through-space conjugation of localised clusters of amide linkages, which could account for the aforementioned surface roughness enhancement, can allow n–π*/π –π * electronic interactions through overlap of their electron clouds in close proximity to form nonconventional luminogens[72], which were lost when these interactions were disrupted upon dissolution to form dilute solutions. It is possible that the strong hydrogen bonding between amides, indicated by FTIR (**Figure 2b**), enhances structural rigidity that reduces non-radiative energy losses. The similar emission profiles of both HDPEAm and LDPEAm (**Figure 5b**) suggests that there are restrictions in conformations in the ensemble distribution of amide clusters that can be formed in spite of the different extents of branching between both polymers. Although such CTE-luminescence has been observed with non-aromatic polyamides such as nylon-6 [73] and polyaminoamides[74-76] with high functional group density, this optical phenomenon was also present with oxidised PEs possessing low degrees of alcohol, carbonyl and ester functionalisation[11, 77]. We thus further investigated the possibility of using the amide-containing HDPEAm as a luminescent additive to HDPE, potentially bringing about cost savings. Mixtures containing different weight ratios of HDPEAm and unfunctionalized HDPE, subjected to homogenisation under applied pressure and heat, still exhibited CTE-luminescence upon irradiation under 390 nm light (**Figure S55**). The clusteroluminescence of the PEAms offer the possibility for upcycling PEs for potential sensing applications, and could also act as intrinsic fluorescent markers to facilitate polymer sorting from mixtures without the need for luminescent marker additives.

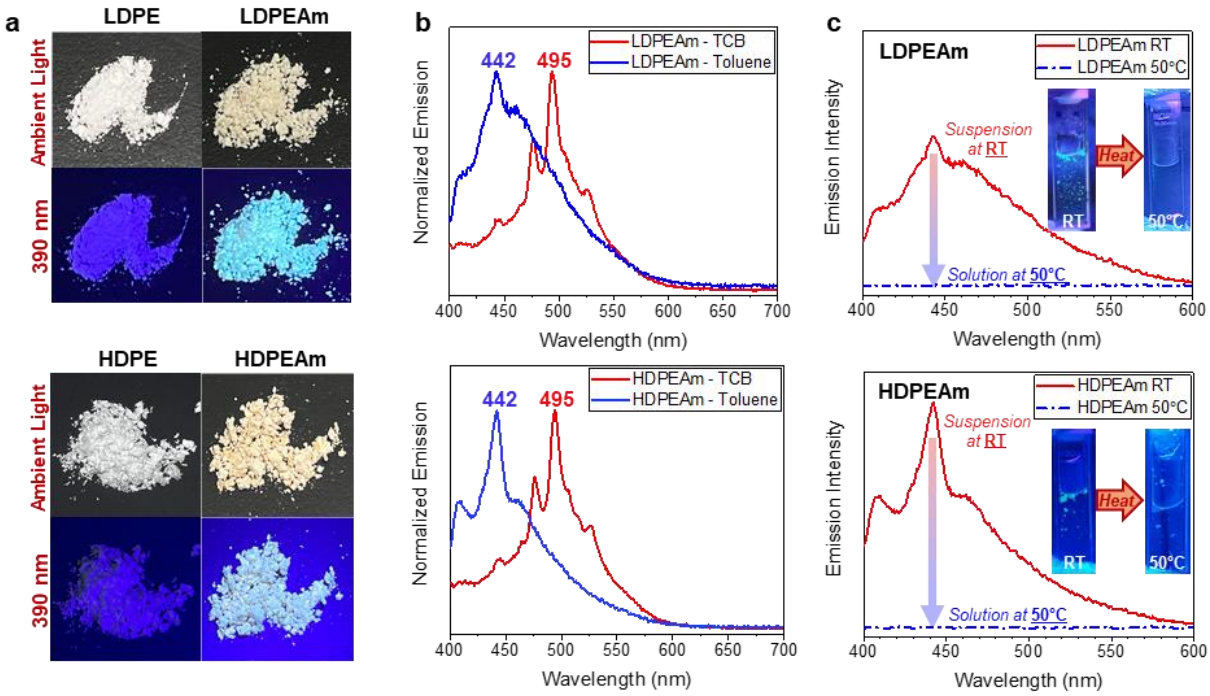


**Figure 5. Non-chromophore luminescence of HDPEAm and LDPEAm. a)** Irradiation of the original PE powders and their in-chain amide-inserted counterparts under ambient lighting and 390 nm. **b)** Stacked normalised emission spectra of LDPEAm (top) and HDPEAm (bottom) in TCB (red) and toluene (blue). **c)** Stacked emission spectra of LDPEAm (top) and HDPEAm (bottom) when suspended in toluene at RT and dissolved at 50 °C ($\lambda_{ex}$ = 390 nm) All emission spectra were recorded at [polymer] = 1 mg/mL.

**Parent PE Structure-dependent Chemical Recyclability**

Chemical recycling of the amide-inserted PEs was evaluated through repeated cycles of polymer hydrolysis and amide reformation. Compared to thermal PE depolymerization, that often occurs at temperatures >700 °C and produces low ethylene selectivity due to random chain scissions,[4] the in-chain amides allow site-selective cleavage to occur under much milder conditions at 130 °C in refluxing aqueous HCl for 24 hours. Successful amide hydrolysis of HDPEAm was observed from the appearance of the distinct $^1$H NMR signals of the α-methylenes to -COOH (triplet centred ~2.38 ppm) and -$NH_2$ (broad peak centred ~3.05 ppm) groups, with a corresponding reduction in the relative intensity of the amide signal (C***H***$_2$-CONH, ~2.15 ppm) (**Figure 6a**). Subsequent reformation of the polyamide (HDPEAm-r) was performed using the neat hydrolysed polymer fragments mediated by titanium(IV) isopropoxide (TIP) at ≤150 °C (see Supporting Information for detailed procedure), as evidenced by the reappearance of the characteristic amide triplet $^1$H NMR signal at 2.15 ppm and quartet at 3.25 ppm. Using the same procedures, we were able to demonstrate acid-mediated polyamide hydrolysis and condensation for an additional two cycles (**Figures S27 – S30**). In all iterations, >90% of the original HDPEAm feed could be retained by mass, with the notable absence of significant additional functionalities on the polymer during repeated hydrolysis-reformation through $^1$H NMR analyses. This outcome contrasted with high-temperature pyrolytic PE recycling where recovery of ethylene for repolymerisation is typically <30 %, with the remainder lost through side product formation from multiple competing decomposition pathways.[78, 79]

Polyamide reformation from HDPEAm largely retained its thermal stability, with decomposition temperature showing a slight increase from 434 °C (HDPEAm) to 442 °C (HDPEAm-r3, after the 3$^{rd}$ cycle of reformation) (**Table 2**). Similarly, $T_m$ was maintained between 110-120 °C throughout 3 cycles of hydrolysis-reformation. Additionally, the reformed polyamides generally possessed improved mechanical properties compared to HDPEAm, with ultimate tensile strength and elongation at break increasing by up to ~48% and ~23% respectively compared to the original HDPEAm (**Figure 6b**). The reformed polyamides were found to exhibit poorer solubility than HDPEAm, which precluded representative high-temperature GPC analyses of their molecular weight and polydispersity. Nonetheless, when taken together, these characterisations suggested the possibility of further extensions of the polymer chains upon repeated amide formation. Compared to mechanical recycling, which inevitably leads to polymer chain scission that compromises on the polymers' material

properties[80], amide reformation potentially allows restoration and even improvements on the thermal and mechanical properties of HDPEAm. Additionally, it offers opportunities to compensate for any loss in polymer mechanical properties resulting from the initial PE amide insertion (**Table 1**), simply by controlling degree of polymerisation of the hydrolysed HDPEAm fragments.

Attempted hydrolysis and amide reformation on LDPEAm resulted in very different outcomes to HDPEAm. Like HDPEAm, hydrolysis of LDPEAm in refluxing HCl resulted in the appearance of the distinct $^1$H NMR signals of the -COOH α-protons (2.38 ppm) and -$NH_2$ (broad peak centred ~3.05 ppm) that were originally not present, accompanied by a decrease in relative intensity of the corresponding amide α-proton signal at 2.23 ppm (**Figure S13**). When the partially hydrolysed polymer was subjected to TIP-mediated amide reformation, we obtained a crosslinked polymer (LDPEAm-r) (68% gel fraction in chloroform) that showed sparing solubility (i.e. excellent solvent resistance) to both 1,1,2,2-tetrachloroethane or 1,2,4-TCB at 130 °C for up to 72 h – conditions that are known to dissolve PE and derivatives[81]. Due to its poor solubility, $^1$H NMR and GPC analyses could not be performed to determine the degree of amide reformation or changes in molecular weight. To further assess the chemical stability of LDPEAm-r, we subjected the polymer to hydrolysis and alcoholysis under forcing thermal and microwave-assisted conditions in the presence of acid or base (**Section S15**). In all cases, no visible polymer dissolution or degradation was detected, suggesting the potential suitability of LDPEAm-r in moderate chemi-resistive applications.

To probe the nature of chemical crosslinking in LDPEAm-r, XPS analyses was performed, and the N1s spectrum was compared with that of the partially-hydrolysed LDPEAm-h and parent LDPEAm prior to attempted chemical recycling. Like LDPEAm, the N1s spectrum of LDPEAm-r showed a single dominant peak with binding energy of 399-400 eV arising from the amide nitrogen atoms (**Section S13, Figure S56**). In contrast, two distinct peaks were evident from the spectrum of partially-hydrolysed LDPEAm-h at 399.8 and 401.3 eV that could be assigned to amides and protonated primary amines respectively.[82] These findings clearly indicated the dominance of amide functionalities in LDPEAm-r from polycondensation of the oligomeric fragments of LDPEAm-h. Additionally, we performed a control experiment by subjecting the unreacted parent LDPE polymer to the same hydrolysis and TIP-mediated reformation reactions used for LDPEAm, which resulted no additional polymer functionalisation or crosslinking (**Figure S35**). These demonstrated that the crosslinking in LDPEAm-r likely resulted from amide reformation.

Compared to LDPEAm, the repolymerised LDPEAm-r showed similar thermal stability with $T_d$ unchanged at 454 °C, though a slight decrease in melting temperature was observed (**Table 2, Figure S38**). Despite crosslink formation, LDPEAm-r was largely amenable to compression moulding, with the resulting dogbone fragments showing small extent of heterogeneity due to non-uniform melting even using a hot press at 260 °C. Nonetheless, the resulting measured tensile properties may be taken as an estimate for comparison against LDPEAm (Table 1). LDPEAm-r had greatly improved polymer ductility, possessing 7.5x and 2.2x increased elongation at break compared to LDPE and LDPEAm respectively as a result of polymer chain interconnection (**Figure 6c**).[83] However, a significant reduction in polymer rigidity was observed, as indicated by the decrease in Young's modulus from 92 MPa in LDPEAm to 27 MPa in LDPEAm-r. This was likely attributable to the decrease in polymer crystallinity upon formation of the crosslinked LDPEAm-r which hindered polymer chain packing, with XRD analysis showing a marked reduction in percentage crystallinity from 43.5% in LDPEAm to 24.8% in LDPEAm-r (**Figure S44**), being similarly reflected in the decrease in $T_c$ observed by DSC (**Table 2**).

**Table 2.** Physical properties of HDPEAm-r and LDPEAm-r after each iteration of repolymerisation[a].

| **Property** | **Repeated HDPEAm recycling** | | | **LDPEAm-r** |
|---|---|---|---|---|
| | **HDPEAm-r1** | **HDPEAm-r2** | **HDPEAm-r3** | |
| $T_c$ /°C [a] | 99.8 | 103.0 | 100.3 | 64.4[d] |
| $T_m$ /°C [a] | 117.5 | 115.8 | 114.8 | 88.2[d] |
| $T_d$ /°C [b] | 438.2 | 438.5 | 441.8 | 454.1 |
| Ultimate tensile strength /MPa [c] | 16.13 ± 0.69 | 16.31 ± 0.56 | 24.29 ± 1.22 | 6.39 |
| Elongation at break /% [c] | 124.7 ± 1.0 | 149.6 ± 10.6 | 144.4 ± 47.9 | 233.2 |
| Max stress at break /MPa [c] | 14.54 ± 0.47 | 14.61 ± 0.85 | 22.36 ± 2.01 | 5.97 |
| Young's Modulus /$10^8$ Pa [c] | 3.03 ± 0.07 | 2.45 ± 0.69 | 2.24 ± 0.12 | 6.39 |

[a]Properties of the parent HDPEAm and LDPEAm used for chemical recyclability are summarised in **Table 1**. Thermal properties of the polymers determined via [a]DSC and [b]TGA

(See Supplementary Information). [b]extrapolated onset temperatures from the TGA curve; [c]Determined from tensile analyses (See Supplementary Information), values are the averages of three repeats; [d] Due to crosslinked nature of LDPEAm-r, exothermic and endothermic peaks in its DSC curve corresponds to the crystallization and melting of residual hydrolysed fragments or loosely crosslinked segments.

The stark differences observed upon attempted chemical recycling of HDPEAm and LDPEAm containing similar extents (~1 mol%) of amide functionalisation, strongly implied that the extent of PE branching could affect its chemical recyclability upon in-chain amide insertion. The amide linkages are likely located randomly on the polymer chains, dependent on the sites of initial carbonyl functionalisation, which has been shown by $^{1}$H NMR to be widely spaced apart and not clustered together (vide supra). With HDPE containing few branches ($^{13}$C NMR (**Figure S34**), it is statistically likely for the amides to be present along the main chain. Amide hydrolysis thus cleaves the polymer into largely linear fragments, which can be recombined to form similarly linear, albeit possibly longer polymer chains, upon subsequent polycondensation (accounting for the observed poorer polymer solubility) (**Figure 6d**). In contrast, the highly branched nature of LDPE (**Figure S33**) allows the amides to be inserted at random sites on both the main chain and branches. When hydrolysis occurs, branched fragments containing multiple reactive termini can be formed (**Figure 6e**). Since the recombination of these fragments can theoretically occur between any accessible carboxylic acid and amine site, amide polycondensation will thus result in scrambling of these oligomeric fragments. It is thus possible that PE chains can be crosslinked by oligomeric fragments that contain multiple reactive termini, to form a crosslinked thermoset-like polymer. At the same time, low molecular weight oligomers may also be formed from recombination of short fragments that can be dissolved in organic solvents, accounting for the moderate gel fractions observed for LDPEAm-r. Although crosslinking can also theoretically occur between any tertiary alcohols present (formed on the LDPE branch points after oxidation) with COOH-containing fragments, we were able to exclude this possibility from their absence on LDPEK as determined by $^{13}$C NMR analysis (**Figures S7 – S8**). These findings thus suggest that insertion of cleavable bonds (e.g. amides) into unreactive PE backbones may only confer chemical recyclability if the parent polymer was largely linear. Though the presence of branches in LDPEAm gives rise to very different material and recyclability outcomes (**Figure 6f**), the ability to transform LDPEAm into a thermoset simply by hydrolysis and

polycondensation offers a convenient and low-cost method to synthesise chemo- and thermo-resistive polyamide thermosets. This contrasts with conventional methods which can involve thermal curing (typically >200 °C)[84] or photocuring using synthetically-challenging monomers[85, 86]. This strategy could also offer an opportunity to tune crosslinking degree and the resulting properties of the thermosets by controlling the feed ratios, and judicious selection from the wide assortment of existing PE precursors with different degrees of branching.

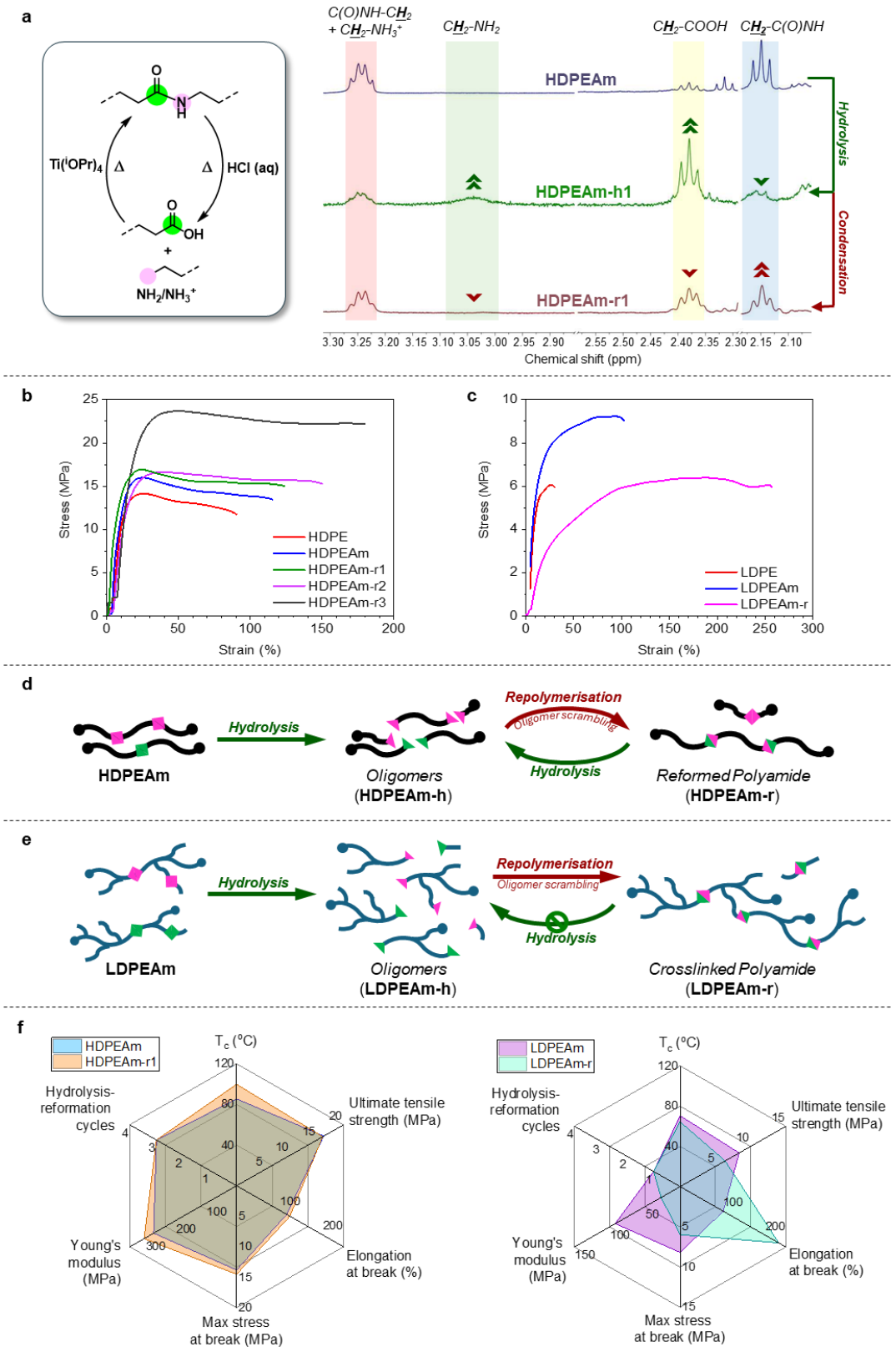


**Figure 6. a)** Stacked partial $^{1}$H NMR spectra of HDPEAm, the acid-hydrolysed and repolymerised products (spectra referenced to 2.38 ppm [C$\underline{H}_2$COOH] for clarity due to differing product solubility in TCE-$d_2$, necessitating different temperatures). **b)** Representative stress-strain curves of HDPE, HDPEAm and the reformed polyamides after successive

iterations of chemical recycling. **c)** Representative stress-strain curves of LDPE, LDPEAm and the crosslinked polyamide. Schematic depiction showing the effects of polymer branches on hydrolysis and condensation of **d)** HDPEAm and **e)** LDPEAm. **f)** Radar plots summarising the differences in material properties and recyclability of HDPEAm (left) and LDPEAm (right) after 1 cycle of amide reformation.

## Conclusions

In conclusion, we have demonstrated how post-synthetic insertion of hydrolysable amide linkages into unreactive PE hydrocarbon backbones can augment a host of diverse physical properties, whilst concurrently introducing a new circular phase into their traditionally linear, unsustainable life cycles. Such amide insertion can occur on different types of PE polymers, with the usage of common, low-cost reagents and green bioderived solvents enhancing its attractiveness for industrial translation. Even a small amount of inserted amides was sufficient to influence polymer self-assembly and interactions through hydrogen bonding and entanglement, in turn enhancing macroscopic material properties such as tensile strength, elongation at break and even surface roughness that led to unexpected enhancement in hydrophobicity compared to the parent PEs. Additionally, the amides enabled through-space electronic interactions that led to formation of non-traditional luminophores that manifested in detectable luminescence in the solid state that was not present in the original PEs. Compared to conventional methods for improving mechanical properties[87], hydrophobicity[88] and conferring fluorescence[89] to PEs through additive incorporation, the ability to confer these properties simply by amide insertion avoids these additional materials, which can complicate waste streams and increase the complexity of recycling. These properties also offer new possibilities for PEs to be used in applications traditionally inaccessible to the parent polymers, such as PTFE replacements or in anti-counterfeiting that exploits the resulting greater hydrophobicity and luminescence respectively, to name a few.

Our study also uncovered the important, but hitherto-overlooked influences of the parent polymer branching structure on chemical recyclability of PE containing randomly-positioned in-chain amides. For HDPE containing low branching, we demonstrated three cycles of repeated amide hydrolysis and reformation could be achieved below 200 °C, without significantly compromising material and thermal stability. In contrast, the presence of amide linkages on the extensively branched structure of LDPE resulted in the formation of a

thermoset-like crosslinked polymer upon hydrolysis and amide reformation, which showed greatly augmented ductility, excellent solvent and chemical resistance. Although the PE resins used in this proof-of-concept study possess relatively low molecular weight, we expect that the findings herein to be also applicable to real-life PE samples of higher molecular weight. Nonetheless, the diverse functional material properties observed herein upon amide insertion *into* PE backbones complement those from appending heteroatom-containing functional groups (e.g. hydroxyl, carbonyl and oximes) *onto* the polymer[15, 33], and provide improved tensile behaviour compared to ester linkage insertion (**Table S5**).[7, 11] Our findings demonstrate the possibility of allowing both recyclability and PE upcycling by post-synthetic insertion of only amide linkages into the polymer backbone, thus providing new perspectives into functional upcycling and engineering circular materials from ubiquitous PE plastics for a more sustainable materials economy.

## Data Availability

The data that support the findings of this study are presented in the Supplementary Information, and are available from the corresponding authors on reasonable request.

## Main References


1. Baker, A. M. E.; Windle, A. H., The effects of branching and fibre drawing on the crystal structure of polyethylene. *Polymer* **2001,** *42* (2), 651-665.
2. Sperati, C. A.; Franta, W. A.; Starkweather, H. W., Jr., The Molecular Structure of Polyethylene. V. The Effect of Chain Branching and Molecular Weight on Physical Properties1. *J. Am. Chem. Soc.* **1953,** *75* (24), 6127-6133.
3. Patel, A. D.; Schyns, Z. O. G.; Franklin, T. W.; Shaver, M. P., Defining quality by quantifying degradation in the mechanical recycling of polyethylene. *Nat Commun.* **2024,** *15* (1), 8733.
4. Kim, S. W.; Kim, Y. T.; Tsang, Y. F.; Lee, J., Sustainable ethylene production: Recovery from plastic waste via thermochemical processes. *Sci. Total Environ.* **2023,** *903*.
5. Tardy, A.; Nicolas, J.; Gigmes, D.; Lefay, C.; Guillaneuf, Y., Radical Ring-Opening Polymerization: Scope, Limitations, and Application to (Bio)Degradable Materials. *Chem. Rev.* **2017,** *117* (3), 1319-1406.
6. Haussler, M.; Eck, M.; Rothauer, D.; Mecking, S., Closed-loop recycling of polyethylene-like materials. *Nature* **2021,** *590* (7846), 423-427.
7. Baur, M.; Mast, N. K.; Brahm, J. P.; Habe, R.; Morgen, T. O.; Mecking, S., High-Density Polyethylene with In-Chain Photolyzable and Hydrolyzable Groups Enabling Recycling and Degradation. *Angew. Chem. Int. Ed. Engl.* **2023,** *62* (45), e202310990.
8. Lu, Y.; Takahashi, K.; Zhou, J.; Nontarin, R.; Nakagawa, S.; Yoshie, N.; Nozaki, K., Synthesis of Long-Chain Polyamides via Main-Chain Modification of Polyethyleneketones. *Angew. Chem. Int. Ed. Engl.* **2024,** *63* (43), e202410849.

9. Ditzler, R. A. J.; King, A. J.; Towell, S. E.; Ratushnyy, M.; Zhukhovitskiy, A. V., Editing of polymer backbones. *Nat Rev Chem* **2023,** *7* (9), 600-615.
10. Kong, D.; Wang, L.; Chen, X.; Xia, W.; Su, L.; Zuo, F.; Yan, Z.; Chen, S.; Wu, J., Chemical-biological degradation of polyethylene combining Baeyer–Villiger oxidation and hydrolysis reaction of cutinase. *Green Chem* **2022,** *24* (5), 2203-2211.
11. Shen, C.; Zhang, Q.; Wei, X.; Ye, P.; Liu, X.; Xu, S.; Wang, Y.-Z., Upcycling of polyethylene waste to biodegradable adhesive and coating via Baeyer-Villiger reaction: A new view on oxidation-fracture mechanism and structure-function relationship. *Polymer* **2024,** *313*, 127689.
12. Lemmens, R.; Vercammen, J.; Van Belleghem, L.; De Vos, D., Upcycling polyethylene into closed-loop recyclable polymers through titanosilicate catalyzed C-H oxidation and in-chain heteroatom insertion. *Nat Commun* **2024,** *15* (1), 9188.
13. N. R. Ciccia; J. X. Shi; S. Pal; M. Hua; K. G. Malollari; C. Lizandara-Pueyo; E. Risto; M. Ernst; B. A. Helms; P. B. Messersmith; Hartwig, J. F., Diverse functional polyethylenes by catalytic amination. *Science* **2023,** *381*, 1433–1440.
14. Zhou, H.; Wang, S.; Huang, H.; Li, Z.; Plummer, C. M.; Wang, S.; Sun, W.-H.; Chen, Y., Direct Amination of Polyethylene by Metal-Free Reaction. *Macromol.* **2017,** *50* (9), 3510-3515.
15. Otten, M.; Klein Gebbink, I.; Schara, P. J.; Tomović, Ž.; Lutz, M.; Bruijnincx, P. C. A.; Thevenon, A., Post-Polymerization Modification of Polyethylene through Photochemical Oximation and Consecutive Ketonization. *Journal of the American Chemical Society* **2025,** *147* (26), 22827-22838.
16. Li, X.; He, Y.; Dong, X.; Ren, X.; Gao, H.; Hu, W., Effects of hydrogen-bonding density on polyamide crystallization kinetics. *Polymer* **2020,** *189*.
17. Puiggalí, J., Aliphatic polyamides (nylons): Interplay between hydrogen bonds and crystalline structures, polymorphic transitions and crystallization. *Polym. Cryst.* **2021,** *4* (4), e10199.
18. Das, A.; Babu, A.; Chakraborty, S.; Van Guyse, J. F. R.; Hoogenboom, R.; Maji, S., Poly(N-isopropylacrylamide) and Its Copolymers: A Review on Recent Advances in the Areas of Sensing and Biosensing. *Adv. Funct. Mater.* **2024,** *34* (37), 2402432.
19. de Witt, J.; Luthe, T.; Wiechert, J.; Jensen, K.; Polen, T.; Wirtz, A.; Thies, S.; Frunzke, J.; Wynands, B.; Wierckx, N., Upcycling of polyamides through chemical hydrolysis and engineered Pseudomonas putida. *Nat. Microbiol* **2025,** *10* (3), 667-680.
20. Češarek, U.; Pahovnik, D.; Žagar, E., Chemical Recycling of Aliphatic Polyamides by Microwave-Assisted Hydrolysis for Efficient Monomer Recovery. *ACS Sustain Chem Eng.* **2020,** *8* (43), 16274-16282.
21. Ngu, J.; Najmi, S.; Selvam, E.; Vance, B.; Yang, P.; Vlachos, D. G., Catalytic deconstruction of organic additive-containing plastics. *Nat. Chem. Eng.* **2025,** *2* (3), 220-228.
22. Hinton, Z. R.; Kots, P. A.; Soukaseum, M.; Vance, B. C.; Vlachos, D. G.; Epps, T. H.; Korley, L. T. J., Antioxidant-induced transformations of a metal-acid hydrocracking catalyst in the deconstruction of polyethylene waste. *Green Chem.* **2022,** *24* (19), 7332-7339.
23. Maddela, N. R.; Kakarla, D.; Venkateswarlu, K.; Megharaj, M., Additives of plastics: Entry into the environment and potential risks to human and ecological health. *J. Environ. Manage.* **2023,** *348*, 119364.
24. Wiesinger, H.; Wang, Z.; Hellweg, S., Deep Dive into Plastic Monomers, Additives, and Processing Aids. *Environ. Sci. Technol.* **2021,** *55* (13), 9339-9351.
25. Teo, J. Y. Q.; Yeung, C. W. S.; Tan, T. T. Y.; Loh, W. W.; Loh, X. J.; Lim, J. Y. C., Benzaldehyde-mediated selective aerobic polyethylene functionalisation with isolated backbone ketones. *Green Chem.* **2022,** *24*, 6287-6294.

26. Bunescu, A.; Lee, S.; Li, Q.; Hartwig, J. F., Catalytic Hydroxylation of Polyethylenes. *ACS Cent. Sci.* **2017,** *3* (8), 895-903.
27. Teo, J. Y. Q.; Tan, M. Y.; Safanama, D.; Chien, S. W.; Jiang, Y.; Queh, L.; Tan, T. T. Y.; Ding, N.; Fam, D. W. H.; Lim, J. Y. C., A cradle-to-cradle approach for successive upcycling of polyethylene to polymer electrolytes to organic acids. *J. Mater. Chem. A* **2024**.
28. Yeung, C. W. S.; Periayah, M. H.; Teo, J. Y. Q.; Goh, E. T. L.; Chee, P. L.; Loh, W. W.; Loh, X. J.; Lakshminarayanan, R.; Lim, J. Y. C., Transforming Polyethylene into Water-Soluble Antifungal Polymers. *Macromol.* **2023,** *56* (3), 815-823.
29. Tang, S.; Seidel, F. W.; Nozaki, K., High Density Polyethylenes Bearing Isolated In-Chain Carbonyls. *Angew. Chem. Int. Ed.* **2021,** *60* (51), 26506-26510.
30. Shi, J. X.; Ciccia, N. R.; Pal, S.; Kim, D. D.; Brunn, J. N.; Lizandara-Pueyo, C.; Ernst, M.; Haydl, A. M.; Messersmith, P. B.; Helms, B. A.; Hartwig, J. F., Chemical Modification of Oxidized Polyethylene Enables Access to Functional Polyethylenes with Greater Reuse. *J. Am. Chem. Soc.* **2023,** *145* (39), 21527-21537.
31. Zhang, K.; Nelson, A. M.; Talley, S. J.; Chen, M.; Margaretta, E.; Hudson, A. G.; Moore, R. B.; Long, T. E., Non-isocyanate poly(amide-hydroxyurethane)s from sustainable resources. *Green Chem.* **2016,** *18* (17), 4667-4681.
32. Song, L.; Zhu, T.; Yuan, L.; Zhou, J.; Zhang, Y.; Wang, Z.; Tang, C., Ultra-strong long-chain polyamide elastomers with programmable supramolecular interactions and oriented crystalline microstructures. *Nat. Commun.* **2019,** *10* (1), 1315.
33. Chen, L.; Malollari, K. G.; Uliana, A.; Sanchez, D.; Messersmith, P. B.; Hartwig, J. F., Selective, Catalytic Oxidations of C-H Bonds in Polyethylenes Produce Functional Materials with Enhanced Adhesion. *Chem* **2021,** *7* (1), 137-145.
34. Lemmens, R.; Vercammen, J.; Van Belleghem, L.; De Vos, D., Upcycling polyethylene into closed-loop recyclable polymers through titanosilicate catalyzed C-H oxidation and in-chain heteroatom insertion. *Nat Commun.* **2024,** *15* (1), 9188.
35. Byrne, F. P.; Jin, S.; Paggiola, G.; Petchey, T. H. M.; Clark, J. H.; Farmer, T. J.; Hunt, A. J.; Robert McElroy, C.; Sherwood, J., Tools and techniques for solvent selection: green solvent selection guides. *Sustain. Chem. Process.* **2016,** *4* (1), 7.
36. Clark, J. H.; Macquarrie, D. J.; Sherwood, J., A quantitative comparison between conventional and bio-derived solvents from citrus waste in esterification and amidation kinetic studies. *Green Chem.* **2012,** *14* (1), 90-93.
37. Granato, A. V.; Santos, A. G.; dos Santos, E. N., p-Cymene as Solvent for Olefin Metathesis: Matching Efficiency and Sustainability. *ChemSusChem* **2017,** *10* (8), 1832-1837.
38. Ye, L.; Thompson, B. C., p-Cymene: A Sustainable Solvent that is Highly Compatible with Direct Arylation Polymerization (DArP). *ACS Macro Lett.* **2021,** *10* (6), 714-719.
39. Satira, A.; Espro, C.; Paone, E.; Calabrò, P. S.; Pagliaro, M.; Ciriminna, R.; Mauriello, F., The Limonene Biorefinery: From Extractive Technologies to Its Catalytic Upgrading into p-Cymene. *Catal.* **2021,** *11* (3).
40. Boardman, H., The Mechanism of Oxidation of p-Cymene. *J. Am. Chem. Soc.* **1962,** *84* (8), 1376-1382.
41. Li, H.; Meng, Y.; Shu, C.; Li, X.; Kiss, A. A.; Gao, X., Innovative Reactive Distillation Process for the Sustainable Synthesis of Natural Benzaldehyde. *ACS Sustain Chem Eng.* **2018,** *6* (11), 14114-14124.
42. Randall, J. C., Carbon-13 NMR of ethylene-1–olefin copolymers: Extension to the short-chain branch distribution in a low-density polyethylene. *J. Polym. Sci. Polym. Phys. Ed.* **1973,** *11* (2), 275-287.
43. Jung, M.; Lee, Y.; Kwak, S.; Park, H.; Kim, B.; Kim, S.; Lee, K. H.; Cho, H. S.; Hwang, K. Y., Analysis of Chain Branch of Polyolefins by a New Proton NMR Approach. *Anal. Chem.* **2016,** *88* (3), 1516-1520.

44. Arroyave, A.; Cui, S.; Lopez, J. C.; Kocen, A. L.; LaPointe, A. M.; Delferro, M.; Coates, G. W., Catalytic Chemical Recycling of Post-Consumer Polyethylene. *J. Am. Chem. Soc.* **2022,** *144* (51), 23280-23285.
45. Li, K.; Chen, X.; Pan, Y.; Min, B.; Ye, E.; Li, S.; Li, Z.; Loh, X. J., Balancing Degradability and Mechanical Strength in Keto Modified Polyethylene through Hydrogen Bonds. *ACS Materials Letters* **2024,** *6* (6), 2259-2266.
46. Pawlak, A., The Entanglements of Macromolecules and Their Influence on the Properties of Polymers. *Macromol. Chem. Phys.* **2019,** *220* (10), 1900043.
47. Ortmann, P.; Lemke, T. A.; Mecking, S., Long-Spaced Polyamides: Elucidating the Gap between Polyethylene Crystallinity and Hydrogen Bonding. *Macromol.* **2015,** *48* (5), 1463-1472.
48. Chen, Z.; Lu, H., Constructing sacrificial bonds and hidden lengths for ductile graphene/polyurethane elastomers with improved strength and toughness. *J. Mater. Chem.* **2012,** *22* (25).
49. Degtyar, E.; Harrington, M. J.; Politi, Y.; Fratzl, P., The Mechanical Role of Metal Ions in Biogenic Protein-Based Materials. *Angew. Chem. Int. Ed.* **2014,** *53* (45), 12026-12044.
50. Jeong, S. H.; Kim, J. M.; Yoon, J.; Tzoumanekas, C.; Kröger, M.; Baig, C., Influence of molecular architecture on the entanglement network: topological analysis of linear, long- and short-chain branched polyethylene melts via Monte Carlo simulations. *Soft Matter* **2016,** *12* (16), 3770-3786.
51. Lu, T.; Chen, Q., Independent gradient model based on Hirshfeld partition: A new method for visual study of interactions in chemical systems. *J. Comput. Chem.* **2022,** *43* (8), 539-555.
52. Lu, T.; Chen, F., Multiwfn: a multifunctional wavefunction analyzer. *J. Comput. Chem.* **2012,** *33* (5), 580-92.
53. Wang, J.; Wolf, R. M.; Caldwell, J. W.; Kollman, P. A.; Case, D. A., Development and testing of a general amber force field. *J. Comput. Chem.* **2004,** *25* (9), 1157-74.
54. Hanwell, M. D.; Curtis, D. E.; Lonie, D. C.; Vandermeersch, T.; Zurek, E.; Hutchison, G. R., Avogadro: an advanced semantic chemical editor, visualization, and analysis platform. *J. Cheminf.* **2012,** *4* (1), 17.
55. Abraham, M. J.; Murtola, T.; Schulz, R.; Páll, S.; Smith, J. C.; Hess, B.; Lindahl, E., GROMACS: High performance molecular simulations through multi-level parallelism from laptops to supercomputers. *SoftwareX* **2015,** *1-2*, 19-25.
56. Bussi, G.; Donadio, D.; Parrinello, M., Canonical sampling through velocity rescaling. *J. Chem. Phys.* **2007,** *126* (1), 014101.
57. Berendsen, H. J. C.; Postma, J. P. M.; Gunsteren, W. F. v.; DiNola, A.; Haak, J. R., Molecular dynamics with coupling to an external bath. *J. Chem. Phys.* **1984,** *81* (8), 3684-3690.
58. Frisch, M. J.; Trucks, G. W.; Schlegel, H. B.; Scuseria, G. E.; Robb, M. A.; Cheeseman, J. R.; Scalmani, G.; Barone, V.; Mennucci, B.; Petersson, G. A.; Nakatsuji, H.; Caricato, M.; Li, X.; Hratchian, H. P.; Izmaylov, A. F.; Bloino, J.; Zheng, G.; Sonnenberg, J. L.; Hada, M.; Ehara, M.; Toyota, K.; Fukuda, R.; Hasegawa, J.; Ishida, M.; Nakajima, T.; Honda, Y.; Kitao, O.; Nakai, H.; Vreven, T.; Montgomery, J. A.; Peralta, J. E.; Ogliaro, F.; Bearpark, M.; Heyd, J. J.; Brothers, E.; Kudin, K. N.; Staroverov, V. N.; Kobayashi, R.; Normand, J.; Raghavachari, K.; Rendell, A.; Burant, J. C.; Iyengar, S. S.; Tomasi, J.; Cossi, M.; Rega, N.; Millam, J. M.; Klene, M.; Knox, J. E.; Cross, J. B.; Bakken, V.; Adamo, C.; Jaramillo, J.; Gomperts, R.; Stratmann, R. E.; Yazyev, O.; Austin, A. J.; Cammi, R.; Pomelli, C.; Ochterski, J. W.; Martin, R. L.; Morokuma, K.; Zakrzewski, V. G.; Voth, G. A.; Salvador, P.; Dannenberg, J. J.; Dapprich,

S.; Daniels, A. D.; Farkas, Ö.; Foresman, J. B.; Ortiz, J. V.; Cioslowski, J.; Fox, D. J., Gaussian 09 Revision E.01. 2009.
59. Yanai, T.; Tew, D. P.; Handy, N. C., A new hybrid exchange–correlation functional using the Coulomb-attenuating method (CAM-B3LYP). *Chem. Phys. Lett.* **2004,** *393* (1-3), 51-57.
60. McLean, A. D.; Chandler, G. S., Contracted Gaussian basis sets for molecular calculations. I. Second row atoms, Z=11–18. *J. Chem. Phys.* **1980,** *72* (10), 5639-5648.
61. Grimme, S.; Hansen, A.; Brandenburg, J. G.; Bannwarth, C., Dispersion-Corrected Mean-Field Electronic Structure Methods. *Chem. Rev.* **2016,** *116* (9), 5105-5154.
62. Zhao, Y.; Truhlar, D. G., The M06 suite of density functionals for main group thermochemistry, thermochemical kinetics, noncovalent interactions, excited states, and transition elements: two new functionals and systematic testing of four M06-class functionals and 12 other functionals. *Theor. Chem. Acc.* **2007,** *120* (1-3), 215-241.
63. Yu, X.; Kong, B.; Yang, X., Molecular Dynamics Study on the Crystallization of a Cluster of Polymer Chains Depending on the Initial Entanglement Structure. *Macromol.* **2008,** *41* (18), 6733-6740.
64. Li, X.; Wang, J.; Yi, G.; Teong, S. P.; Chan, S. P.; Zhang, Y., From waste plastic to artificial lotus leaf: Upcycling waste polypropylene to superhydrophobic spheres with hierarchical micro/nanostructure. *Appl. Catal. B: Environ.* **2024,** *342*.
65. Ensikat, H. J.; Ditsche-Kuru, P.; Neinhuis, C.; Barthlott, W., Superhydrophobicity in perfection: the outstanding properties of the lotus leaf. *Beilstein J. Nanotechnol.* **2011,** *2*, 152-61.
66. Extrand, C. W., Water Contact Angles and Hysteresis of Polyamide Surfaces. *J. Colloid Interface Sci.* **2002,** *248* (1), 136-142.
67. Ciccia, N. R.; Shi, J. X.; Pal, S.; Hua, M.; Malollari, K. G.; Lizandara-Pueyo, C.; Risto, E.; Ernst, M.; Helms, B. A.; Messersmith, P. B.; Hartwig, J. F., Diverse functional polyethylenes by catalytic amination. *Science* **2023,** *381* (6665), 1433-1440.
68. Mańko, D.; Zdziennicka, A.; Jańczuk, B., Surface tension of polytetrafluoroethylene and its wetting by aqueous solution of some surfactants and their mixtures. *Appl. Surf. Sci.* **2017,** *392*, 117-125.
69. Moradi, R.; Karimi-Sabet, J.; Shariaty-Niassar, M.; Koochaki, M., Preparation and Characterization of Polyvinylidene Fluoride/Graphene Superhydrophobic Fibrous Films. *Polymers* **2015,** *7* (8), 1444-1463.
70. Lohmann, R.; Cousins, I. T.; DeWitt, J. C.; Gluge, J.; Goldenman, G.; Herzke, D.; Lindstrom, A. B.; Miller, M. F.; Ng, C. A.; Patton, S.; Scheringer, M.; Trier, X.; Wang, Z., Are Fluoropolymers Really of Low Concern for Human and Environmental Health and Separate from Other PFAS? *Environ. Sci. Technol.* **2020,** *54* (20), 12820-12828.
71. Zhang Yuan, W.; Zhang, Y., Nonconventional macromolecular luminogens with aggregation-induced emission characteristics. *J. Polym. Sci., Part A: Polym. Chem.* **2017,** *55* (4), 560-574.
72. Zhang, H.; Zhao, Z.; McGonigal, P. R.; Ye, R.; Liu, S.; Lam, J. W. Y.; Kwok, R. T. K.; Yuan, W. Z.; Xie, J.; Rogach, A. L.; Tang, B. Z., Clusterization-triggered emission: Uncommon luminescence from common materials. *Mater. Today* **2020,** *32*, 275-292.
73. Chen, X.; Yang, T.; Lei, J.; Liu, X.; Zhao, Z.; Xue, Z.; Li, W.; Zhang, Y.; Yuan, W. Z., Clustering-Triggered Emission and Luminescence Regulation by Molecular Arrangement of Nonaromatic Polyamide-6. *J. Phys. Chem. B* **2020,** *124* (40), 8928-8936.
74. Wang, D.; Imae, T., Fluorescence Emission from Dendrimers and Its pH Dependence. *J. Am. Chem. Soc.* **2004,** *126* (41), 13204-13205.

75. Lee, W. I.; Bae, Y.; Bard, A. J., Strong Blue Photoluminescence and ECL from OH-Terminated PAMAM Dendrimers in the Absence of Gold Nanoparticles. *J. Am. Chem. Soc.* **2004,** *126* (27), 8358-8359.
76. Lin, Y.; Gao, J.; Liu, H.; Li, Y., Synthesis and Characterization of Hyperbranched Poly(ether amide)s with Thermoresponsive Property and Unexpected Strong Blue Photoluminescence. *Macromol.* **2009,** *42*, 3237-3246.
77. Zhao, Y.; Long, J.; Zhuang, P.; Ji, Y.; He, C.; Wang, H., Transforming polyethylene and polypropylene into nontraditional fluorescent polymers by thermal oxidation. *Journal of Materials Chemistry C* **2022,** *10* (3), 1010-1016.
78. Mastral, J. F.; Berrueco, C.; Ceamanos, J., Modelling of the pyrolysis of high density polyethylene: Product distribution in a fluidized bed reactor. *J. Anal. Appl. Pyrolysis.* **2007,** *79* (1), 313-322.
79. Levine, S. E.; Broadbelt, L. J., Detailed mechanistic modeling of high-density polyethylene pyrolysis: Low molecular weight product evolution. *Polym. Degrad. Stab.* **2009,** *94* (5), 810-822.
80. Zhang, J.; Hirschberg, V.; Goecke, A.; Wilhelm, M.; Yu, W.; Orfgen, M.; Rodrigue, D., Effect of mechanical recycling on molecular structure and rheological properties of high-density polyethylene (HDPE). *Polymer* **2024,** *297*, 126866.
81. Whiteley, K. S.; Heggs, T. G.; Koch, H.; Mawer, R. L.; Immel, W., Polyolefins. In *Ullmann's Encyclopedia of Industrial Chemistry*, 2000.
82. Yu, B.; Wang, X.; Qian, X.; Xing, W.; Yang, H.; Ma, L.; Lin, Y.; Jiang, S.; Song, L.; Hu, Y.; Lo, S., Functionalized graphene oxide/phosphoramide oligomer hybrids flame retardant prepared via in situ polymerization for improving the fire safety of polypropylene. *RSC Adv* **2014,** *4* (60), 31782-31794.
83. Song, F.; Li, Z.; Jia, P.; Zhang, M.; Bo, C.; Feng, G.; Hu, L.; Zhou, Y., Tunable "soft and stiff", self-healing, recyclable, thermadapt shape memory biomass polymers based on multiple hydrogen bonds and dynamic imine bonds. *J. Mater. Chem. A* **2019,** *7* (21), 13400-13410.
84. Li, M.; Dingemans, T. J., Synthesis and characterization of semi-crystalline poly(decamethylene terephthalamide) thermosets. *Polymer* **2017,** *108*, 372-382.
85. Sathyan, A.; Hayward, R. C.; Emrick, T., Ring-Opening Polymerization of Allyl-Functionalized Lactams. *Macromol.* **2018,** *52* (1), 167-175.
86. He, W.; Tao, Y.; Wang, X., Functional Polyamides: A Sustainable Access via Lysine Cyclization and Organocatalytic Ring-Opening Polymerization. *Macromol.* **2018,** *51* (20), 8248-8257.
87. Awan, M. O.; Shakoor, A.; Rehan, M. S.; Gill, Y. Q., Development of HDPE composites with improved mechanical properties using calcium carbonate and NanoClay. *Physica B.* **2021,** *606*, 412568.
88. Chu, X.; Zhang, P.; Shi, S.; Liu, Y.; Feng, W.; Zhou, N.; Li, J.; Shen, J., Hydrophobic self-cleaning micro-nano composite polyethylene-based agricultural plastic film with light conversion and abrasion resistance. *Colloids Surf. A: Physicochem. Eng.* **2023,** *658*, 130621.
89. Arenas-Vivo, A.; Beltrán, F. R.; Alcázar, V.; de la Orden, M. U.; Martinez Urreaga, J., Fluorescence labeling of high density polyethylene for identification and separation of selected containers in plastics waste streams. Comparison of thermal and photochemical stability of different fluorescent tracers. *Mater. Today Commun.* **2017,** *12*, 125-132.

## Acknowledgements

The authors are grateful to Dr Derrick Fam (IMRE) and Ms Chien Sheau Wei (IMRE) for use of the microtensile tester. The authors also acknowledge Dr. Debbie Seng for her assistance with XPS analyses. Financial support of this project from A*STAR under its RIE2025 Manufacturing, Trade and Connectivity (MTC) Programmatic Funding (Grant No. M22K9b0049) is gratefully acknowledged.

## Author contributions

J. Y. C. L and Z. L conceived the concept. A. O. and J. Y. C. L jointly devised the experimental procedures and A. O. and J. J. M. P. performed all the synthesis and recyclability experiments. L. W. W. assisted with all material fabrication, WCA and tensile analysis. J. Y. Q. T assisted with all thermal and IR characterisations. X. Q. K assisted with all AFM characterisation and analysis. T. T. Y. T assisted with all XRD characterisation and analysis, L. K. performed all the computational studies and L.Q. performed high temperature GPC analyses. J. Y. C. L., A. O. and J. J. M. P. wrote the manuscript with inputs from all the authors. A. O. and J. J. M. P. contributed equally to this work.

## Competing Interests

A patent has been filed by the Institute of Materials Research and Engineering (IMRE), A*STAR based on the findings reported herein.